ELSEVIER

Journal of Molecular Catalysis B: Enzymatic 8 (2000) 3–15

JOURNAL OF MOLECULAR CATALYSIS B: ENZYMATIC

www.elsevier.com/locate/molcatb

Spectroscopic and magnetochemical studies on the active site copper complex in galactose oxidase

Mei M. Whittaker [a], Christopher A. Ekberg [a], James Peterson [c], Mariana S. Sendova [b], Edmund P. Day [b], James W. Whittaker [a,*]

[a] *Department of Biochemistry and Molecular Biology, Oregon Graduate Institute of Science and Technology, P.O. Box 91000, Portland, OR 97291-1000, USA*

[b] *Department of Physics, Emory University, Atlanta, GA 30322, USA*

[c] *Department of Chemistry, Carnegie Mellon University, Pittsburgh, PA 55455, USA*

Dedicated to Prof. Hans Duine in celebration of his contributions to the field of quinoprotein enzymology

Abstract

Galactose oxidase is a radical copper oxidase, an enzyme making use of a covalently modified tyrosine residue as a free radical redox cofactor in alcohol oxidation catalysis. We report here a combination of spectroscopic and magnetochemical studies developing insight into the interactions between the active site Cu(II) and two distinct tyrosine ligands in the biological complex. One of the tyrosine ligands (Y495) is coordinated to the Cu(II) metal center as a phenolate in the resting enzyme and serves as a general base to abstract a proton from the coordinated substrate, thus activating it for oxidation. The structure of the resting enzyme is temperature-dependent as a consequence of an internal proton equilibrium associated with this tyrosine that mimics this catalytic proton transfer step. The other tyrosine ligand (Y272) is covalently crosslinked to a cysteine residue forming a tyrosine–cysteine dimer free radical redox site that is required for hydrogen atom abstraction from the activated substrate alkoxide. The presence of the free radical in the oxidized active enzyme results in formation of an EPR-silent Cu(II) complex shown by multifield magnetic saturation experiments to be a diamagnetic singlet arising from antiferromagnetic exchange coupling between the metal and radical spins. A paramagnetic contribution observed at higher temperature may be associated with thermal population of the triplet state, thus permitting an estimate of the magnitude of the isotropic exchange coupling ($J > 200$ cm^{-1}, $JS_1 \cdot S_2$) in this complex. Structural correlations and the possible mechanistic significance of metal–radical coupling in the active enzyme are discussed.

Keywords: Free radical; Copper; EPR; Magnetic susceptibility; Proton transfer

1. Introduction

Enzymatic catalysis has emerged in this century as the ultimate refinement of reaction chemistry, combining extraordinary catalytic rate enhancements with exquisite selectivity. The subtlety of enzyme design, now revealed in hundreds of atomic resolution protein crystal structures, has inspired synthetic chemists aiming to reproduce the essential features of these biological active sites in small molecule models.

* Corresponding author. Tel.: +1-503-690-1065; fax: +1-503-690-1464; e-mail: jim@bmb.ogi.edu

1381-1177/00/$ - see front matter
PII: S1381-1177(99)00072-7

However, in spite of exciting developments in recent years, biological catalysts are still unsurpassed by their synthetic analogs, and in general it appears to be much easier to imitate structure than to reproduce function. Success may ultimately depend on deeper insight into the catalytic principles expressed in enzyme complexes, reaching beyond the atomic coordinates available from crystallography to understand both their dynamical implications in protein motion and their consequences at the level of electronic structure.

The structural elements from which proteins form their catalytic complexes are deceptively simple: an alphabet of 20 L-amino acids, each contributing unique chemical and structural characteristics. Proteins can extend this basic 20-letter alphabet by covalent modification of protein side chains, generating novel structures with essential new properties and reactivities. Nearly two decades ago, the work of Duine [1–4] and others [5–7] brought to light a new class of modifications that confer on the protein the ability to directly participate in oxidation–reduction chemistry through the formation of redox active amino acid side chains [8]. Post-translational covalent modification of tryptophan and tyrosine residues leads to the formation of a variety of quinonoid derivatives (pyrroloquinoline quinone (PQQ) [1–4]; tryptophan tryptophylquinone (TTQ) [5]; topa quinone (TPQ) [6]; lysine tyrosylquinone (LTQ) [7]; etc.) that can serve as prosthetic groups in catalysis. These redox active amino acid side chains give rise to special reactivities characteristic of quinoproteins and are often associated with free radical mechanisms of catalysis [9,10].

A distinct type of modification is represented by the free radical enzyme, galactose oxidase [11]. The unique features of galactose oxidase redox site have emerged from a combination of biochemical [12] and spectroscopic [13–18] studies that have revealed a free radical-coupled copper complex in the active enzyme. This remarkably stable free radical complex was overlooked in earlier spectroscopic studies which principally focussed on a catalytically inactive form of the enzyme lacking the radical [19]. Detailed characterization of the radical in the oxidized enzyme has led to assignment of the radical to a modified or perturbed tyrosine residue in the protein based on resonance Raman spectra [14] and analysis of the unusual EPR spectrum of the protein free radical and isotopic labelling experiments [13]. Crystallography has subsequently revealed an unusual feature of the active site metal center [20,21] (Fig. 1). One of the two tyrosine ligands coordinating the active site metal ion (Y272) is found to be covalently crosslinked at a position *ortho* to the phenolic oxygen to the $S\gamma$ of a cysteine residue (C228). This tyrosine–cysteine dimer is restricted to one-electron reactivity, making it distinct from other quinocofactors. Model studies on thioether substituted phenols and their metal complexes [22–26] as well as advanced spectroscopic experiments (resonance Raman [14,16], ENDOR [17], high field EPR [18]) on the enzyme have confirmed that this modified tyrosine is redox active in the protein.

The active site of galactose oxidase thus brings together a core of catalytic features including three essential elements: the redox active metal ion, which interconverts between Cu(II) and Cu(I) in the course of reaction; a simple tyrosine phenolate (Y495), coordinated to the Cu(II) metal ion in the resting enzyme at ambient temperature and serving as a proton coupling element of the catalytic complex; and

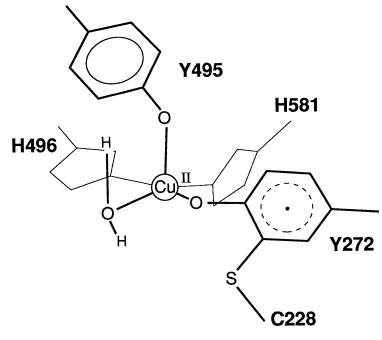

Fig. 1. The active site of galactose oxidase (based on crystallographic coordinates PDB ID 1GOG [Refs. [20,21]]).

the Y272–C228 tyrosine–cysteine dimer which serves as a one-electron redox cofactor. This phenoxyl forms the free radical-coupled copper complex in the active enzyme.

The interactions between the metal ion and the two tyrosines is of central importance in the catalytic mechanism of galactose oxidase [27]. We report here on an intrinsic instability of the active site structure resulting from a transition in Cu(II)-Y495 phenolate interactions in the inactive enzyme. Multifield magnetic susceptibility measurements further explore the electronic interactions between the metal and phenoxyl redox orbitals in the active enzyme complex.

2. Materials and methods

2.1. Biological materials

Galactose oxidase (E.C. 1.1.3.9) was purified from *Dactylium dendroides* (ATCC 46032) cultures as previously described [12] and converted to the catalytically active form by oxidation with 50 mM $K_3Fe(CN)_6$ followed by desalting over a Bio Rad Laboratories BioGel P-30 column equilibrated with 50 mM sodium phosphate buffer pH 7 [12]. For spectroscopic experiments the reductively inactivated enzyme was prepared in the same fashion with 50 mM $K_4Fe(CN)_6$ as reductant. For susceptibility studies reduction was accomplished by addition of one equivalent of sodium ascorbate to the enzyme under an argon atmosphere. All spectroscopic and magnetochemical measurements were performed on protein samples transferred to 50 mM sodium phosphate buffer pH 7 in D_2O (99 atom% ^2H) by dilution/concentration cycles in an ultrafiltration cell. This reduces background hysteresis in the magnetization data resulting from nuclear susceptibility of slowly relaxing solvent protons and reduces vibrational overtone absorption in the NIR. Samples for variable temperature absorption measurements were prepared in 50% (v/v) glycerol glassing solvent and injected into a cell formed from a pair of quartz disks separated by a silicone rubber spacer with a circular bore holding 120 μl of solution. Susceptibility samples were prepared in quartz buckets, degassed by pump/purge cycling with argon to remove dissolved oxygen, and frozen slowly in liquid nitrogen. Molecular oxygen is a common paramagnetic ($S = 1$) impurity in susceptibility experiments. Protein concentration was determined by optical absorption measurements, using the previously reported molar extinction coefficient ($\varepsilon_{280} = 1.05 \times 10^5\ M^{-1}\ cm^{-1}$) [28]. All reagents for preparation of culture media and buffers were from commercial sources and were used without purification.

2.2. Spectroscopic instrumentation

Optical absorption spectra were recorded on a Varian Instruments Cary 5E UV–vis–NIR absorption spectrometer interfaced with a microcomputer for data acquisition. To avoid condensation artifacts in the NIR, the sample chamber was purged with dry nitrogen gas. Variable temperature measurements were made using a Cryo Industries model RC-152 VT (5–300 K) vapor immersion optical cryostat, with a dual sample holder. Temperature at the sample was measured using a calibrated silicon diode sensor and a Lakeshores Cryotronics model 330 temperature controller. Samples were cooled (< 1 K/min) in a stream of helium gas at atmospheric pressure, and absorption measurements were referenced to a solvent blank prepared in parallel with the protein sample and mounted in tandem on the sample block. EPR spectra were recorded on a Bruker ER300 EPR spectrometer equipped with a Bruker ER4116 DM bimodal cavity and an Oxford Instruments ESR900 helium flow cryostat. Spin quantitation was performed as previously described [12].

2.3. Multifield magnetization experiments

Multifield saturation magnetization studies made use of a fully automated Quantum Design

Superconducting Susceptometer (Quantum Design, San Diego, CA). programmed to collect data at several fixed fields over the temperature range 2–200 K as previously described [29,30]. Theoretical powder magnetization curves were calculated and the experimental data fit using commercial software (WEB Research, Edina, MN) to analyze the data.

3. Results

3.1. Temperature-dependent active site structure

Galactose oxidase undergoes distinctive color changes on cooling to liquid nitrogen temperature (77 K). The characteristic intense green color of the radical-containing active enzyme (AGO) is replaced by a straw yellow at low temperature, and the blue color of the radical-free inactive enzyme (IAGO) turns to red under similar conditions. The latter complex can be prepared in 50% glycerol glassing solvent, allowing the spectral changes associated with this transformation to be measured over the entire transition region and thus permitting a more detailed analysis.

The optical absorption spectrum of IAGO progressively shifts as the temperature is varied from ambient (300 K) to cryogenic (20 K) reflecting a smooth interconversion between limiting high- and low-temperature forms (Fig. 2). At ambient temperature, the active site Cu(II) center gives rise to transitions at 350, 440 and 635 nm, while the low temperature spectrum has features at 345 and 532 nm. Between these limits, the intermediate spectra maintain an isosbestic at 380 nm. These spectral changes are independent of the buffer used, and appear to reflect an internal temperature-dependent equilibrium in the active site metal complex. The temperature profile of the absorption changes at 650 nm is shown in the lower panel of Fig. 2. Below 150 K, there is a small-amplitude increase in intensity which has been fit to a linear function of temperature and subtracted from the entire data set. The most dramatic feature of the profile is the relatively abrupt appearance (near 150 K) of a transition region over which the majority of the spectral change occurs. This transition region spans approximately 200 K and has a sigmoidal profile suggesting simple interconversion between two discrete limiting structures, one stable at lower temperature and the other becoming stabilized as the temperature is raised:

$$\mathrm{L} \overset{K_{eq}}{\rightleftarrows} \mathrm{H} \tag{1}$$

where L and H represent the structures stable at low and high temperature and K_{eq} is the temperature-dependent equilibrium constant that determines the partitioning between these limiting forms at a given temperature.

The thermochemical parameters associated with this type of transition can be estimated from a van't Hoff analysis of the spectral data. Defining K_{eq} in terms of the fractional conversion (f) between the limiting forms using the absorption intensity as a measure of the composition of the sample ($f = (\Delta A(T)/(A_L - A_H))$):

$$K_{eq} = f/(1-f) = [\mathrm{H}]/[\mathrm{L}] \tag{2}$$

Since the total absorption A at a given wavelength is the sum of weighted fractional contributions

$$A(T) = (1-f)A_L + (f)A_H \tag{3}$$

the equilibrium constant may be written in terms of absorbance:

$$K_{eq} = (A(T) - A_L)/(A_H - A(T)) \tag{4}$$

with the limiting absorbance values (A_L and A_H) being determined by least-squares analysis of the transition data at a given wavelength. Fig. 3 shows the results of analysis of the IAGO data, allowing estimates of the van't Hoff enthalpy and entropy ($\Delta H_{vH} = 4.9$ kcal/mol; $\Delta S_{vH} = 19$ cal/mol K). The solid line in Fig. 2 indicates the quality of the fit over the transition region.

The interconversion of structures implied by this analysis predicts that distinct ground states

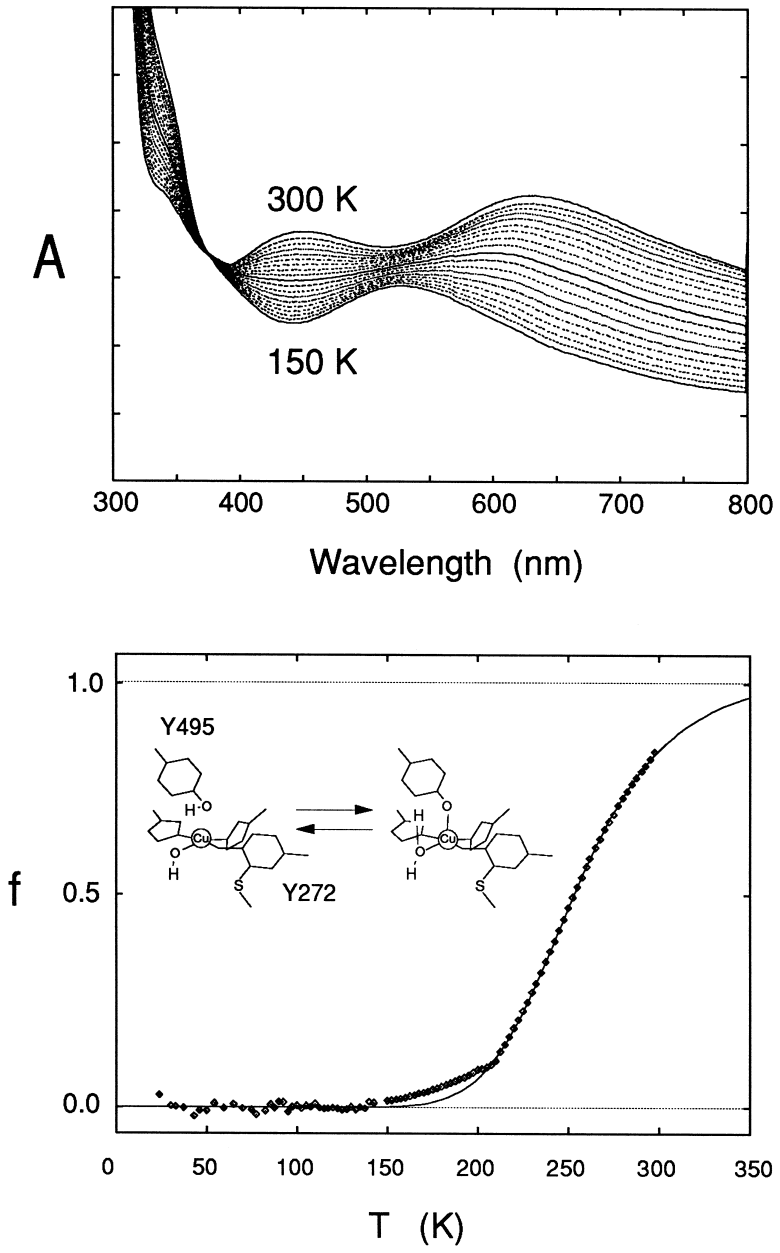

Fig. 2. Variable temperature optical spectra for IAGO. (Top) Optical absorption spectra recorded for IAGO (0.9 mM protein in 50 mM potassium phosphate buffer pH 7, 1 mm path length) in 50% glycerol glassing solvent between 150 and 300 K in 8 K intervals. (Bottom) Normalized 650 nm absorption profile for IAGO between 20 and 300 K after subtraction of low temperature linear dependence from entire dataset as described in the text. *Insert* models the thermal transition in terms of internal proton transfer from coordinated solvent (H_2O) to tyrosine Y495 phenolate.

are associated with the two limiting forms. EPR spectra recorded for IAGO at cryogenic and ambient temperatures are shown in Fig. 4. The low temperature (20 K) EPR spectrum has a relatively large Cu hyperfine splitting ($a_{||} = 179$ G) compared to the ambient temperature (298 K) solution spectrum ($a_{||} = 127$ G). This decrease in copper nuclear hyperfine coupling may

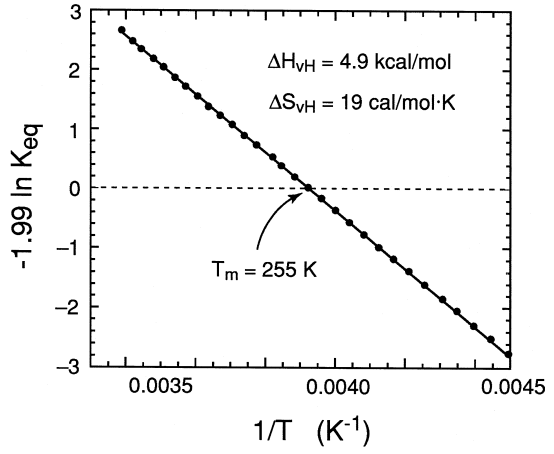

Fig. 3. van't Hoff analysis of IAGO transition. Linear regression of the normalized experimental data with respect to the van't Hoff equation $(-RT \ln K_{eq} = \Delta S_{vH} - \Delta H_{vH}/T)$ yield estimates of the thermochemical parameters ($\Delta H_{vH} = 4.9$ kcal/mol, $\Delta S_{vH} = 19$ cal/mol K) with a midpoint for the transition $T_m = 255$ K.

reflect greater covalent delocalization in the ambient temperature complex. In addition to the decreased hyperfine interaction, there is a slight shift in the parallel component of the *g*-tensor for the Cu(II) ion ($g_{\|} = 2.29$ (20 K) vs. 2.27 (298 K)) that likely reflects a change in the orbital wavefunctions and splittings in the metal valence shell.

The low temperature optical spectrum for ligand free enzyme resembles the spectra observed for anion complexes of IAGO [15], leading to identification of the low temperature structure as a hydroxide complex. Anion binding has been shown to be associated with displacement of a tyrosinate ligand (leading to loss of the 450 nm phenolate-to-Cu(II) ligand-to-metal charge transfer (LMCT) absorption) and uptake of a single proton by a base with $pK_a > 9$ assigned to the unmodified tyrosine ligand Y495 in the active site complex [15]. Mutagenesis of tyrosine to phenylalanine (Y495F) has been shown to eliminate proton uptake [31], consistent with this interpretation. A temperature-dependent thermal equilibrium between hydroxide and aquo complexes accounts for these observations and implies a facile pathway for transfer of a solvent proton to tyrosine, which can be understood from the crystal structure showing water and tyrosine occupy adjacent positions in the metal complex [20,21]. In the ambient temperature structure of the resting enzyme, water is bound in the pseudoaxial position associated with the longest M–L bond distance (2.81 Å). The Cu–O(Y495) bond distance is slightly shorter (2.56 Å) [20,21]. Although hydrogens are not resolved in protein structures, the heavy atom positions are consistent with the structure shown in Fig. 1, having a water proton oriented to permit hydrogen bonding to the Y495 phenolate oxygen. Analysis of this model suggests a 2–3 Å hydrogen bond could be accommodated, defining a proton transfer coordinate for catalytic movements in the active site. The proposed transition between aquo- and hydroxide-complexes is illustrated in the *Insert* of Fig. 2.

The mechanistic significance of this proton transfer coordinate is shown in Fig. 4. In the absence of crystallographic characterization of the galactose oxidase substrate complex, coordinating anions may serve as models for exoge-

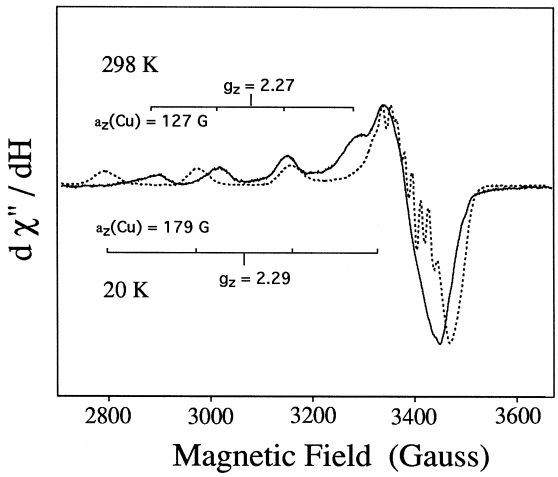

Fig. 4. Groundstates of the IAGO complex at cryogenic and ambient temperatures monitored by EPR spectroscopy. IAGO (50 μM in 50 mM sodium phosphate buffer, pH 7) in solution containing 50% glycerol, 1 mm path length. (——) 290 K spectrum; (– – –) 20 K spectrum. (Instrumental parameters: Microwave frequency, 9.76 GHz; microwave power, 0.5 mW (20 K) or 10 mW (298 K); modulation frequency, 100 kHz; modulation amplitude, 10 G).

nous ligand interactions. Anions (acetate, azide) are known to replace the solvent in the active site, forming pyramidal complexes [20,21]. The substrate complex may thus be modelled by conservative substitution of water by a primary alcohol under the constraint of stereospecific *pro-S* hydrogen abstraction from the substrate 6-hydroxymethyl group [32] by the Y272 phenoxyl implying a structure similar to that shown in Fig. 5. Coordination of the substrate hydroxyl to the metal cation will initially lead to a dramatic acidification of the hydroxylic proton. (For comparison, alcohols coordinated to Zn(II) are acidified by at least ten log units with a reported $pK_a = 7.2$ (25°C) [33].) In this orientation, the substrate may be hydrogen bonded to the Y495 phenolate. This hydrogen bond defines a proton transfer coordinate in the active site. Transfer of the hydroxylic proton from substrate alcohol to protein phenolate will lead to a change in geometry at the metal center, driven by the changing interactions with the two ligands involved in the reaction. Relatively weak pseudoaxial interactions with the substrate hydroxyl are replaced by strong equatorial interactions with alkoxide, while tyrosine phenolate interactions are replaced by a weak pseudoaxial phenolic perturbation. This change in geometry is the origin of the spectral changes observed for the aquoenzyme complex in variable temperature spectroscopy. Proton abstraction is likely to be an essential initial step in galactose oxidase catalysis, activating the substrate for redox. The low energy barrier expected for the proton shift implies that these two limiting structures will be in rapid equilibrium, the relative stabilities determining the extent to which the ionized substrate is available for subsequent reaction steps. This implies a fairly subtle tuning of the active site that we believe is reflected in the thermal conversion of aquo/hydroxo forms and the observation that the conversion is just approaching completion at the physiological temperature range. The thermochromic color changes observed for the active enzyme imply a similar isomerization in the radical copper complex.

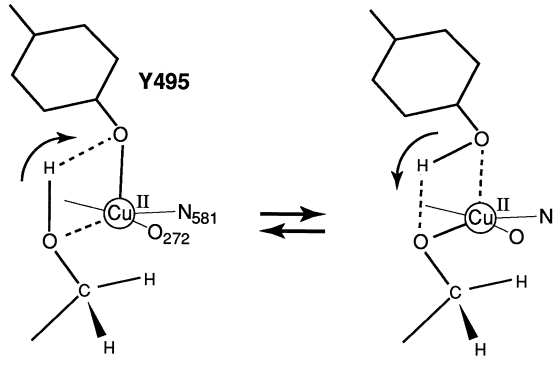

Fig. 5. Proton transfer coordinate for substrate activation by galactose oxidase. Transfer of the hydroxylic proton from the coordinated substrate alcohol (left) to the bound phenolate oxygen of tyrosine Y495 results in displacement of tyrosine from the metal complex (Cu–oxygen stretch) and contraction of the alkoxide–Cu(II) bond.

3.2. Electronic interactions in the radical copper active site

One of the most distinctive features of the active enzyme complex is the electronic coupling of the free radical ligand (Y272 phenoxyl) with the Cu(II) metal ion. These interactions give rise to the unusual absorption spectra of the active enzyme complex, and also account for the absence of an EPR signal from this form of the enzyme [11,12]. Both the protein radical and Cu(II) ion have a single unpaired electron in their valence shells resulting in a spin doublet ($S = 1/2$) electronic ground state which are individually paramagnetic and EPR active. The Cu(II) resonance is observed in the IAGO complex, and the free radical EPR signal can be detected in the oxidized apoenzyme. The absence of EPR spectra for the active enzyme complex is consistent with antiferromagnetic exchange coupling of radical and metal spins leading to a diamagnetic, EPR silent ground state (Fig. 6) with a paramagnetic triplet state at higher energy [12]. The singlet–triplet splitting defines the magnitude of the exchange coupling

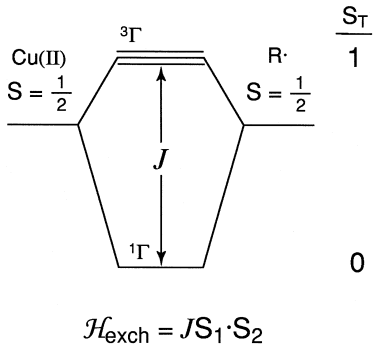

Fig. 6. Exchange coupling diagram for the free radical coupled copper complex of active galactose oxidase. Antiferromagnetic exchange coupling leads to stabilization of a diamagnetic EPR-silent singlet ($S_T = 0$) ground state, with the paramagnetic triplet ($S_T = 1$) state at higher energy.

(J) given by the Heisenberg isotropic exchange Hamiltonian:

$$\mathcal{H}_{exch} = JS_1 \cdot S_2 \quad (5)$$

where S_1 and S_2 are local spin operators and J is the exchange coupling constant. In principle, the population of the excited triplet may be detected by EPR spectroscopy. However, if the zero field splittings within the non-Kramers multiplet are larger than the microwave quantum no transitions will be observed. No EPR resonances are observed for AGO in either parallel or perpendicular microwave polarizations other than those arising from the minority Cu(II) and free radical impurities which are also present at low temperature. The absence of an EPR signal implies electronic coupling within the complex but is not definitive regarding the nature of the coupling.

Magnetic susceptibility provides a sensitive approach to detecting the paramagnetic components in a sample [29,30]. This nonresonant technique overcomes the limitations of spectroscopic detection of paramagnetic species and allows the effects of temperature and magnetic field perturbations to be systematically explored through multifield, variable temperature magnetization measurements. The results of multifield measurements on redox-activated galactose oxidase are shown in Fig. 7 (Top). The magnetization profile plotted in Fig. 7A in terms of the saturation parameter $\beta H/kT$ has the characteristic form of a simple Curie paramagnet but the asymptotic magnetization at the saturation limit is significantly less than predicted for an $S = 1/2$ ground state. The majority of this contribution arises from a fraction of the enzyme which is unable to be oxidized to the radical-containing active enzyme complex. This fraction is estimated at approximately 17% based on spin quantitation of the Cu(II) EPR signal in this sample. Using this value and the average g-value (g_{av}) for the Cu(II) ground state measured in EPR (2.112) a theoretical magnetization curve can be calculated (Fig. 7A). The close correspondence between experiment and theory, especially at the lower temperature range, confirms that the only paramagnetic contribution in the active enzyme at low temperature arises from the minority Cu(II) species. The absence of other paramagnetic contributions in magnetic fields from 1.375 to 5.5 T demonstrates that the free radical coupled copper complex has a dia-

Fig. 7. Multifield saturation magnetization studies of galactose oxidase complexes. (A) Magnetization of active galactose oxidase plotted vs. $\beta H/kT$. The sample contained 320 nmol of protein. The top solid line indicates the expected signal were the entire protein in the $S = 1/2$ ground state with $g_{av} = 2.112$ as seen by EPR. The fit to the data indicates 54 nmol (17%) of the sample was in a spin $S = 1/2$ ground state. Data were collected at fields of 5.500 T (▲), 2.750 T (■), and 1.375 T (●) over the temperature range from 2 K to 200 K. (B) The same data and fit to the data shown in panel (A) are plotted as μ^2_{eff} vs. temperature. The high temperature data indicates a contribution from an antiferromagnetically coupled dimer of $S = 1/2$ spins with $J > 200$ cm^{-1} ($JS_1 \cdot S_2$) in addition to the ground state $S = 1/2$ already described in (A). (C) Magnetization of reduced galactose oxidase plotted vs. $\beta H/kT$. The sample contained 280 nmol of protein. The top solid line indicates the expected signal were the entire protein in the $S = 1/2$ ground state with $g_{av} = 2.112$ as seen by EPR. The fit to the data indicates 220 nmol (79%) of the sample was in a spin $S = 1/2$ ground state. Data were collected at fields of 5.500 T (▲), 2.750 T (■), and 1.375 T (●) over the temperature range from 2 to 200 K. (D) The same data and fit to the data as shown in panel (C) are plotted as μ^2_{eff} vs. temperature. The high temperature data indicates the absence of any paramagnetic component other than the spin $S = 1/2$ ground state as seen in (C).

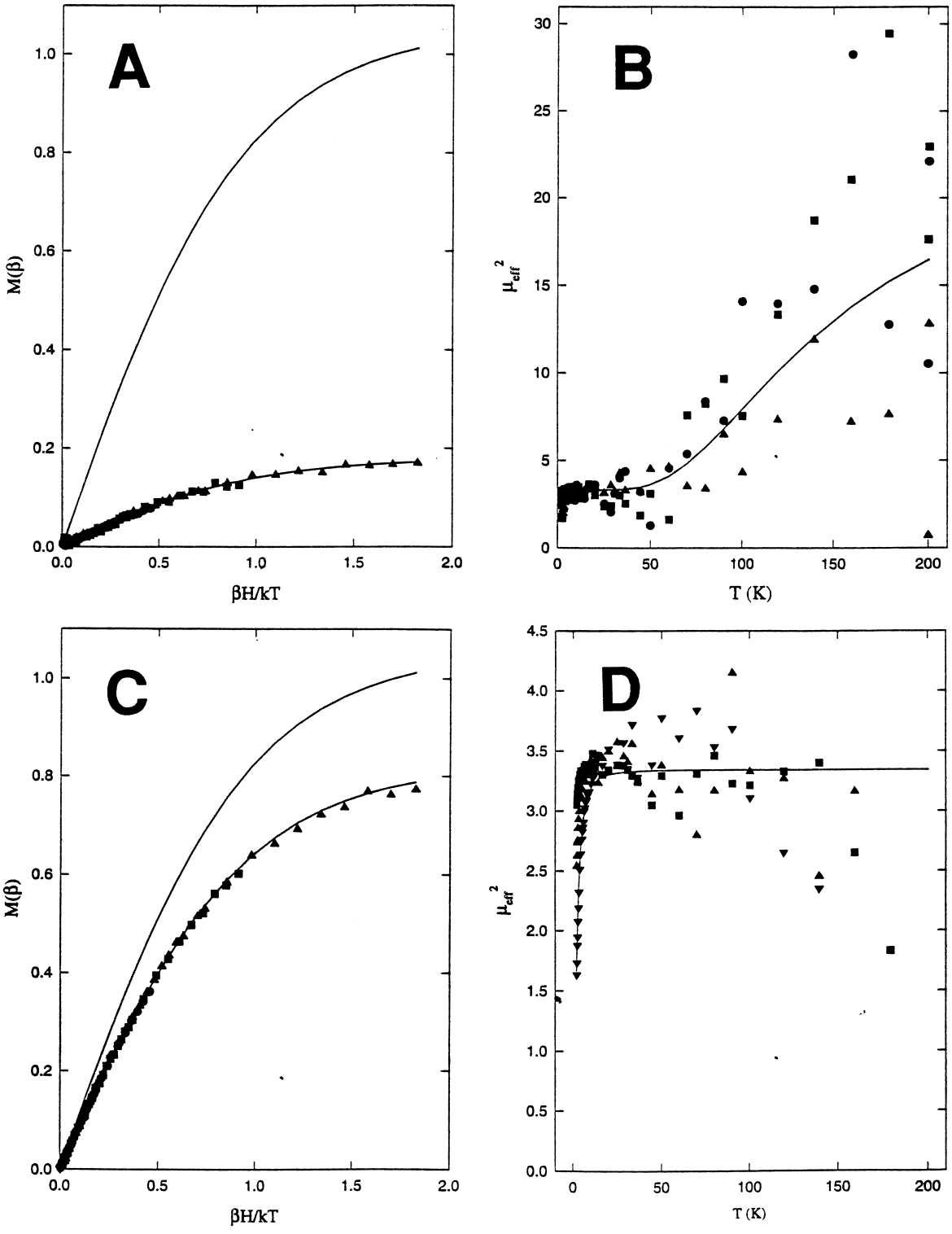
A
M(β)
βH/kT
B
μ_{eff}^2
T (K)
C
M(β)
βH/kT
D
μ_{eff}^2
T (K)

magnetic ground state and thus exhibits antiferromagnetic exchange coupling between radical and copper spins. The deviations between the theoretical line and the experimental data increase somewhat at higher temperatures, as can be more clearly shown by plotting the effective magnetic moment $(\mu_{\text{eff}})^2$ as a function of temperature (Fig. 7B). The growth in the excess magnetic moment as the temperature is raised is consistent with population of a low-lying paramagnetic state. The trend toward higher magnetic moment in increasing magnetic fields is characteristic of a Zeeman perturbation within a non-Kramers triplet state for which the angular momentum is quenched in the absence of a magnetic field by zero field splittings that remove the multiplet degeneracies. Admixture of zero-field states by the magnetic field progressively unquenches the angular momentum, which is reflected in the field-dependence of the magnetic moment. The data shown are not sufficient to determine the magnitude of the exchange coupling accurately but imply a lower limit of about 200 cm^{-1} for the singlet–triplet splitting due to moderately strong antiferromagnetic coupling within the complex.

Magnetization studies on the reductively inactivated Cu(II) enzyme prepared by ascorbate reduction are shown in Fig. 7 (Bottom) for comparison. In this case, the multifield saturation data are fit cleanly to a Curie paramagnet $S = 1/2$ with $g_{\text{av}} = 2.112$ quantitating to 79% of the active sites as determined by complementary EPR characterization of the sample (Fig. 7C). The deviations from Curie behavior that are characteristic of a spin-coupled ground state are absent from this sample, as is clearly shown in Fig. 7D where the high-temperature deviations have the opposite sign and lack any consistent field dependence.

The form of the temperature dependence observed for the magnetization behavior is different from that observed for chemical isomerization of the IAGO enzyme complex, particularly with respect to the lower energy over which the magnetization develops and the relatively broad profile. This makes it unlikely that the growing magnetization arises from ground state ferromagnetism in a higher temperature isomer, although it does not completely rule out that possibility. More likely, the isomerization would not significantly alter the electronic coupling between radical and copper spins, although the coupling to the Y495 phenolate will change depending on its protonation state.

In the natural magnetic orbital picture [34], spatial overlap between half-occupied orbitals on two paramagnetic fragments is the key feature leading to stabilization of the singlet ground state of the complex. The origin of the electronic coupling in galactose oxidase should therefore relate to orbital overlaps between MOs containing the unpaired electrons on the metal and phenoxyl free radical. In Cu(II) electronic structure, spatial quantization of the highest valence orbital (the metal redox orbital) is determined by the strongest (and weakest) interactions in the complex. The energy of the complex is minimized if this half-occupied orbital is directed at the strongest antibonding ligand directions. In a tetragonal complex, these directions are associated with the equatorial ligand positions and define a $d_{x^2-y^2}$ orbital groundstate for Cu(II). In lower symmetry the same principles apply, although the description of the SOMO as a simple cubic d-orbital component becomes progressively less accurate. Based on the crystal structure [20,21], the strongest ligand perturbations in the protein complex will be associated with the two histidines (H496, H581) and tyrosine (Y272), with the trans H496–Y272 interactions defining one component of the equatorial ligand field. The form of the EPR signal from Cu(II) in both aquo and hydroxo complexes of IAGO ($g_{\|} > g_{\perp} > 2$) is characteristic of a $d_{x^2-y^2}$ orbital ground state [11]. The distribution of the unpaired electron in a thioether-substituted phenoxyl radical has been determined both experimentally and computationally [18]. The unpaired electron is localized in the pi-system molecular orbital having contributions from valence p_z atomic orbitals on the

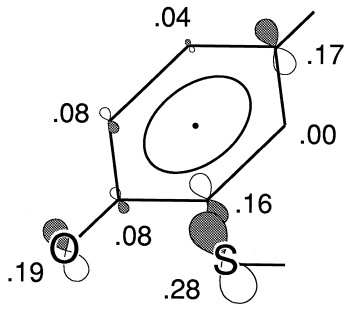

Fig. 8. Unpaired electron distribution in the ground state of the *S*-methyl substituted phenoxyl free radical. The atomic orbital coefficients of the highest-lying occupied MO were calculated using spin unrestricted density functional methods. The size of the p_z orbitals are scaled to reflect relative contributions to the molecular radical.

exocyclic oxygen (0.19), the exocyclic sulfur (0.28) with lesser contributions from the ring carbons in the positions ortho and para to the phenoxyl oxygen (Fig. 8).

Depending on their relative orientations, the interacting magnetic orbitals may have direct sigma overlaps, leading to substantial mixing and antiferromagnetic exchange. Otherwise, the magnetic orbitals will be weakly interacting or orthogonal, leading to weak antiferromagnetic or ferromagnetic coupling in the complex. A more detailed analysis of phenolate–metal coordination in galactose oxidase is required to address these questions. In general, phenolate coordination may be defined in terms of a M–O bond distance and two angles, theta (θ) and tau (τ) (Fig. 9). θ represents the angle between C–O and O–M bond vectors while τ is the dihedral or torsion angle of the M–O vector

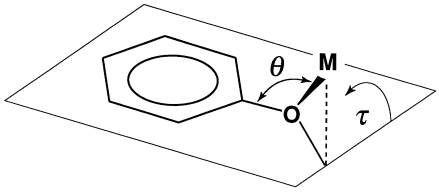

Fig. 9. Coordination modes for tyrosine-metal interactions. In addition to the M–O bond distance, two angles are required to uniquely specify the geometry of the phenolate complex, the ∠C–O–M bond angle (θ) and the dihedral or torsion angle (τ) that determines the rotation of the M–O vector out of the plane of the aromatic ring.

Table 1
Geometric parameters for tyrosinate coordination in galactose oxidase[a]

	d_{M-O}	θ (°)	τ (°)
Y495	2.56	105	53
Y272	1.91	127	−72

[a] Based on crystallographic coordinates reported in PDB ID 1GOG [Refs. [20,21]].

defined relative to the ring plane. A value of the angle τ near 90° (perpendicular coordination) implies strong sigma p_z overlap of the oxygen valence shell (in which the unpaired electron resides) with the metal d-orbital set whereas tau near 0° (parallel coordination) implies pi interactions will dominate. Both of the tyrosine ligands in galactose oxidase have a strong perpendicular tendency (Table 1), particularly Y272 ($\tau = -72°$) that may be expected to result in strong electronic coupling between copper and the free radical, indirectly reflected in the antiferromagnetic exchange interactions. The geometric arrangement of phenoxyl and metal orbitals (Fig. 10) appears favorable for antiferromagnetic coupling, with the spin-occupied Op_z of the phenoxyl pi-system oriented to permit

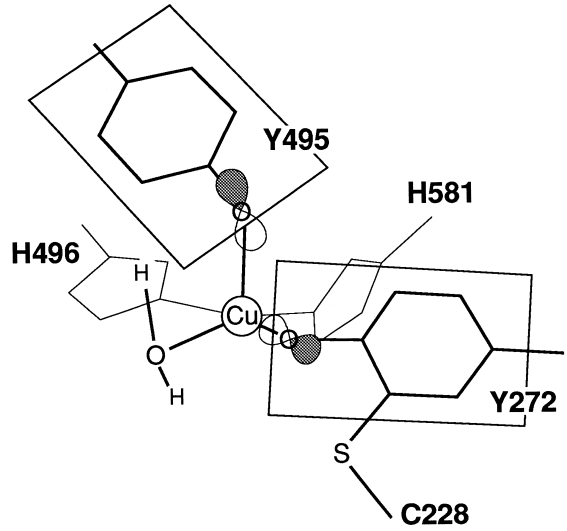

Fig. 10. Orientation of tyrosine ligands in the galactose oxidase copper complex. The p_z orbitals of the aromatic pi-systems lie perpendicular to the ring planes emphasized here.

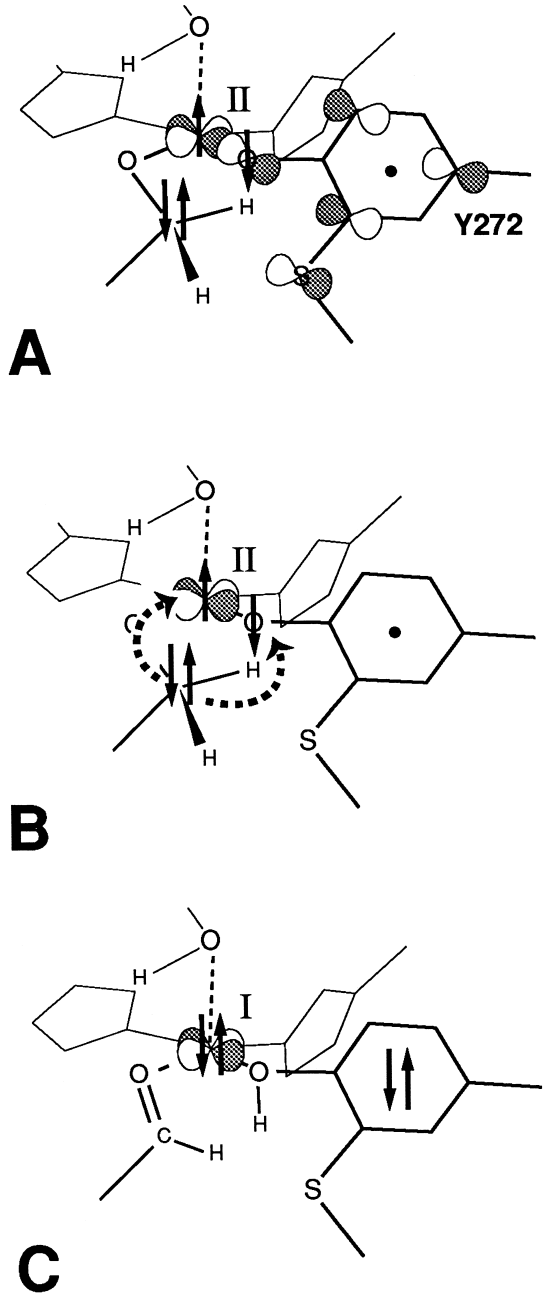

Fig. 11. Spin selection rules for redox chemistry in the free radical coupled Cu(II) complex in galactose oxidase. (A) Singlet substrate coordinated to antiferromagnetically coupled radical copper complex. (B) Pauli principle constraint on initial inner sphere electron transfer to Cu(II) and polarized hydrogen atom transfer to the Y272 phenoxyl. (C) Singlet complex of product aldehyde with Cu(I) [$3d^{10}$] and Y272 phenol.

strong sigma overlaps. Experimentally, antiferromagnetic coupling is observed, and magnetism thus provides useful information on the interactions between the redox orbitals in the oxidized complex. The exchange coupling between radical and metal spins found in these experiments for the biological active site is similar in magnitude to the antiferromagnetic exchange interactions reported for a spin-label free radical copper complex ($J > 450$ cm^{-1}) [35]. The crystal structure of that complex shows the nitroxyl oxygen (on which the unpaired electron is localized) is directly coordinated to the Cu(II) metal center [36].

Radical–copper interactions may play a role in the catalytic redox mechanism of galactose oxidase through spin selection rules for chemistry (Fig. 11). In the course of turnover, the substrate (a closed shell molecule having a singlet ground state) is converted to a singlet closed shell product by reaction with a free-radical Cu(II) complex, whose overlapping orbital components give rise to an antiferromagnetic alignment of electronic spins. Inner sphere electron transfer from the alkoxide substrate to Cu(II) will be constrained by the Pauli principle to select the antiparallel spin, leaving a ketyl radical having molecular polarization that, if it persists, would permit hydrogen atom transfer to the phenoxyl without relaxation of the spins. This requirement on spin chemistry becomes important for chemical reaction rates faster than the relaxation time of the electronic spins, which can be as long as seconds for organic free radicals.

4. Conclusions

Thermal instability of the active site complex results in a structural transition at low temperatures, mapping out a proton transfer coordinate that is expected to be important in the catalytic mechanism of galactose oxidase. Electronic coupling between the Y272 phenoxyl and the Cu(II) metal center stabilize a diamagnetic singlet ground state as a consequence of moderately strong ($J \geq 200$ cm^{-1}) antiferromagnetic

exchange coupling in the free radical copper complex. This interaction may be significant in correlating spins for rapid two-electron redox chemistry in the active site.

Acknowledgements

Support for this research from the National Institutes of Health (GM32394 to E.P.D. and GM46749 to J.W.W.) is gratefully acknowledged.

References

[1] J.A. Duine, J. Frank, J.K. van Zeeland, FEBS Lett. 108 (1979) 443.
[2] J.A. Duine, J. Frank, P.E. Verwiel, Eur. J. Biochem. 108 (1980) 187.
[3] J.A. Duine, Eur. J. Biochem. 200 (1991) 271.
[4] J.A. Duine, Biofactors 2 (1989) 87.
[5] W.S. McIntire, FASEB J. 8 (1994) 513.
[6] S.M. Janes, D. Mu, D. Wemmer, A.J. Smith, S. Kaur, D. Maltby, A.L. Burlingame, J.P. Klinman, Science 248 (1990) 981.
[7] S.W. Wang, M. Mure, K.F. Medzihradszky, A.L. Burlingame, D.E. Brown, A.J. Smith, H.M. Kagan, J.P. Klinman, Science 273 (1996) 1078.
[8] J.P. Klinman (Ed.), Redox Active Amino Acids in Biology, Methods Enzymol., Vol. 258, Academic Press, New York, 1995.
[9] J. Stubbe, Annu. Rev. Biochem. 58 (1989) 257.
[10] J. Stubbe, Biochemistry 27 (1988) 3893.
[11] J.W. Whittaker, in: H. Sigel, A. Sigel (Eds.), Metal Ions in Biological Systems, Vol. 30, Marcel Dekker, Basel, 1994, p. 315.
[12] M.M. Whittaker, J.W. Whittaker, J. Biol. Chem. 263 (1988) 6074.
[13] M.M. Whittaker, J.W. Whittaker, J. Biol. Chem. 265 (1990) 9610.
[14] M.M. Whittaker, V.L. DeVito, S.A. Asher, J.W. Whittaker, J. Biol. Chem. 264 (1989) 7104.
[15] M.M. Whittaker, J.W. Whittaker, Biophys. J. 64 (1993) 762.
[16] M.L. McGlashen, D.D. Eads, T.G. Spiro, J.W. Whittaker, J. Phys. Chem. 99 (1995) 4918.
[17] G. Babcock, M.K. El-Deeb, P.O. Sandusky, M.M. Whittaker, J.W. Whittaker, J. Am. Chem. Soc. 114 (1992) 3727.
[18] G. Gerfen, B.F. Bellew, R.G. Griffen, D.J. Singel, C.A. Ekberg, J.W. Whittaker, J. Phys. Chem. 100 (1997) 16739.
[19] D.J. Kosman, in: R. Lontie (Ed.), Copper Proteins and Copper Enzymes, Vol. 2, CRC Press, Boca Raton, FL, 1985, p. 1.
[20] N. Ito, S.E.V. Phillips, C. Stevens, Z.B. Ogel, M.J. McPherson, J.N. Keen, K.D.S. Yadav, P.F. Knowles, Nature 350 (1991) 87.
[21] N. Ito, S.E.V. Phillips, K.D.S. Yadav, P.F. Knowles, J. Mol. Biol. 238 (1994) 794.
[22] M.M. Whittaker, Y.-Y. Chuang, J.W. Whittaker, J. Am. Chem. Soc. 115 (1993) 10029.
[23] M.M. Whittaker, W.R. Duncan, J.W. Whittaker, Inorg. Chem. 35 (1996) 382.
[24] S. Itoh, K. Hirano, A. Furuta, M. Komatsu, Y. Ohshiro, A. Ishida, S. Takamuku, T. Kohzuma, N. Nakamura, S. Suzuki, Chem. Lett. Jpn. (1993) 2099.
[25] S. Itoh, S. Takayama, R. Arakawa, A. Furuta, M. Komatsu, A. Ishida, S. Takamuku, S. Fukuzumi, Inorg. Chem. 36 (1997) 1407.
[26] D. Zurita, I. Gautier-Luneau, S. Menage, J.-L. Pierre, E. Saint-Aman, J. Biol. Inorg. Chem. 2 (1997) 46.
[27] M.M. Whittaker, J.W. Whittaker, Pure Appl. Chem. (1998), in press.
[28] D.J. Kosman, M.J. Ettinger, R.E. Weiner, E.J. Massaro, Arch. Biochem. Biophys. 165 (1974) 456.
[29] E.P. Day, T.A. Kent, P.A. Lindahl, E. Munck, W.J. Orme-Johnson, H. Roder, A. Roy, Biophys. J. 52 (1987) 837.
[30] E.P. Day, Methods Enzymol. 227 (1993) 437.
[31] M.P. Reynolds, A.J. Baron, C.M. Wilmot, E. Vincombe, C. Stevens, S.E.V. Phillips, P.F. Knowles, M.J. MacPherson, J. Biol. Inorg. Chem. 2 (1998) 327.
[32] A. Maradufu, G.M. Cree, A.S. Perlin, Can. J. Chem. 49 (1971) 3429.
[33] E. Kimura, I. Nakamura, T. Koike, M. Shionoya, Y. Kodama, T. Ikeda, M. Shiro, J. Am. Chem. Soc. 116 (1994) 4764.
[34] O. Kahn, in: R.D. Willett, D. Gatteschi, O. Kahn (Eds.), Magneto-Structural Correlations in Exchange Coupled Systems, NATO ASI Series C, Vol. 140, (1998), D. Reidel Publishing, Boston, MA, p. 37.
[35] Y.Y. Lim, R.S. Drago, Inorg. Chem. 11 (1972) 1334.
[36] M.H. Dickman, R.J. Doedens, Inorg. Chem. 20 (1981) 2677.